

NEAR-AMBIENT SOLID POLYMER FUEL CELL

FINAL REPORT

IN-44-CR
10008

Period of Performance from
January 21, 1993 to July 20, 1993

CONTRACT NO. NASW-4788

Submitted by

G. L. Holleck

EIC Laboratories, Inc.
111 Downey Street
Norwood, Massachusetts 02062

N94-34279

Unclas

G3/44 0010008

Submitted to

NASA Headquarters
300 E Street, SW
Washington, DC 20546

August 10, 1993

(NASA-CR-195939) NEAR-AMBIENT
SOLID POLYMER FUEL CELL Final
Report, 21 Jan. - 20 Jul. 1993
(EIC) 38 p

CONTENTS

<u>Section</u>		<u>Page</u>
	PROJECT SUMMARY	v
1.0	INTRODUCTION	1
2.0	PROJECT OBJECTIVE	2
3.0	PERFORMED RESEARCH AND DEVELOPMENT	2
3.1	Development of Integral Electrode-Membrane Units	2
	3.1.1 General Background and Approach	2
	3.1.2 Fabrication of Electrode-Membrane Structures	3
	3.1.3 Characterization of Electrode-Membrane Structures.....	5
3.2	Fuel Cell Performance Evaluation	7
	3.2.1 Experimental Conditions.....	7
	3.2.2 Fuel Cell test Results.....	15
3.3	Discussion and Conclusions.....	30
4.0	REFERENCES	31

ILLUSTRATIONS

<u>Figure</u>		<u>Page</u>
1	Illustration of a solid polymer membrane fuel cell.....	2
2	Illustration of platinum deposition by electroplating	5
3	Cross-section of an integral Nafion-platinum electrode unit after two impregnation-reduction steps	6
4	Scanning electron micrograph (back scatter mode) showing the cross-section of an integral Nafion-platinum electrode unit after two impregnation-reduction steps	6
5	Scanning electron micrograph showing the surface of an integral Nafion-platinum electrode unit after two impregnation-reduction steps.....	8
6	Cyclic voltammogram of an integral platinum-Nafion membrane fuel cell electrode. Two impregnations. Sweep rate = 20 mV/s.....	8
7	Surface of a carbon supported platinum-Nafion structure (Type A).....	9
8	Cross section of a carbon supported platinum-Nafion structure (Type A). Upper picture, secondary electron image 35° angle; lower picture, back scatter image	10
9	X-ray analysis of the carbon-reconstituted Nafion layer.....	11
10	X-ray analysis of the Nafion membrane about 10 μm from the carbon layer-Nafion interface.....	11
11	Cyclic voltammogram of an integral platinized carbon-Nafion (Type A). Sweep rate = 20 mV/s.....	12
12	Scanning electron micrograph showing the surface of an integral platinized carbon electrode-Nafion structure	12
13	Cross-section of an integral platinized carbon electrode-Nafion structure	13
14	Elemental intensity for Pt, C and F of the electrode-membrane cross section shown in Fig. 13	13
15	Cyclic voltammogram of an integral platinized carbon-Nafion structure (Type B). Sweep rate = 20 mV/s.....	14
16	Illustration of the test cell (exploded view).....	14
17	Illustration of the test cell allowing variation of cell stack compression	15
18	Schematic illustration of the fuel cell test station.....	16
19	Potential-current plot for fuel cell I. 30°C, 2.0 atm H ₂ and O ₂	16

ILLUSTRATIONS
(continued)

<u>Figure</u>		<u>Page</u>
20	Current changes at a constant cell potential of 0.5V as a function of dehydration and rehydration of the Nafion membrane. 50°C, 1.3 atm H ₂ , 1.3 atm O ₂ , O ₂ purge rates: 0 to 220 min; 100 cm ³ /min; 220 to 385 min; 0 cm ³ /min; 385 to 500 min; 5 cm ³ /min. Cell resistance measured by current interruption	19
21	Extended fuel cell operation at 0.5V without gas humidification 30°C 1.3 atm H ₂ , 1.3 atm O ₂ , O ₂ purge 5 cm ³ /min	19
22	Potential-current plot for fuel cell II. 50°C, 1.3 atm H ₂ and O ₂	20
23	Potential-current behavior of a fuel cell with integral Nafion-platinum electrodes operating at 20°C on unhumidified gas. 2 atm H ₂ and O ₂ ; a = cell voltage, b = anode polarization, c = cathode polarization and d = cell resistance	22
24	Potential-current behavior of a fuel cell with integral Nafion-platinum electrodes operating at 20°C on unhumidified gas. 1.3 atm H ₂ and O ₂ ; a = cell voltage, b = anode polarization, c = cathode polarization and d = cell resistance	22
25	Potential-current behavior of a fuel cell with integral Nafion-platinum electrodes operating at 20°C on unhumidified gas. 2 atm H ₂ and air (airflow 60 cm ³ /min.); a = cell voltage, b = anode polarization, c = cathode polarization and d = cell resistance	23
26	Potential-current behavior of a fuel cell with integral Nafion-platinum electrodes operating at 20°C on unhumidified gas. 1.3 atm H ₂ and air (airflow 60 cm ³ /min.); a = cell voltage, b = anode polarization, c = cathode polarization and d = cell resistance.....	23
27	Current and membrane resistance during platinum dehydration of an integral Nafion-electrode unit upon potentiostatic fuel cell operation on unhumidified gas. Cell voltage 0.55V; T = 50°C; 1.3 atm H ₂ without bleed; 1.3 atm O ₂ ; 120 cm ³ /min. bleed	25
28	Current and membrane resistance during self hydration of an integral Nafion-platinum electrode unit upon potentiostatic fuel cell operation. Cell voltage 0.55V; T = 20°C; 1.3 atm H ₂ ; 1.3 atm O ₂ ; gas bleed 7 cm ³ /min. at t >30 min.....	25
29	Current voltage behavior of a carbon supported platinum-Nafion structure (Type A). 20°C, 1.3 atm H ₂ and O ₂ . a, cell voltage; b, anode polarization and c, cathode polarization	27
30	Current voltage behavior of a carbon supported platinum-Nafion structure (Type B). 20°C, 2.0 atm H ₂ and O ₂ . a, cell voltage; b, anode polarization and c, cathode polarization	27

ILLUSTRATIONS
(continued)

Figure		Page
31	Current voltage behavior of a carbon supported platinum-Nafion structure (Type B). 50°C, 1.3 atm H ₂ and O ₂ . a, cell voltage; b, anode polarization and c, cathode polarization	28
32	Current voltage behavior of a carbon supported platinum-Nafion structure (Type B). 20°C, 1.3 atm H ₂ and O ₂ . a, cell voltage; b, anode polarization and c, cathode polarization	28
33	Cell current and resistance at a constant cell voltage of 0.55V during dehydration of a carbon supported platinum-Nafion structure (Type B). 50°C, 1.3 atm H ₂ and O ₂ . O ₂ flow rate = 160 cm ³ /min	29
34	Cell current and resistance at a constant cell voltage of 0.55V during self rehydration of a carbon supported platinum-Nafion structure (Type B). 20°C, 1.3 atm H ₂ and O ₂ . O ₂ bleed rate = 10 cm ³ /min after 75 min	29

PROJECT SUMMARY

Fuel cells are extremely attractive for extraterrestrial and terrestrial applications because of their high energy conversion efficiency without noise or environmental pollution. Among the various fuel cell systems the advanced polymer electrolyte membrane fuel cells based on sulfonated fluoropolymers (e.g., Nafion[®]) are particularly attractive because they are fairly rugged, solid state, quite conductive, of good chemical and thermal stability and show good oxygen reduction kinetics due to the low specific adsorption of the electrolyte on the platinum catalyst. The proton exchange membrane fuel cell (PEMFC) exhibits its best performance at higher temperatures, e.g., 80 to 100°C and at elevated reactant pressure, e.g., 5 atm with well humidified hydrogen and oxygen or air. The gas conditioning and control functions necessary for optimum operation, are responsible for the fact that the cell stack is a vital but only small part of a complete power generating system. For larger fixed installations this approach may be advantageous to minimize cost. It precludes, however, the use of fuel cells for smaller and mobile applications.

The objective of this program is to develop a solid polymer fuel cell which can efficiently operate at near ambient temperatures without ancillary components for humidification and/or pressurization of the fuel or oxidant gases. During the Phase I effort we fabricated novel integral electrode-membrane structures where the dispersed platinum catalyst is precipitated within the Nafion ionomer. This resulted in electrode-membrane units without interfacial barriers permitting unhindered water diffusion from cathode to anode.

The integral electrode-membrane structures were tested as fuel cells operating on H₂ and O₂ or air at 1 to 2 atm and 10 to 50°C without gas humidification. We demonstrated that cells with completely dry membranes could be self started at room temperature and subsequently operated on dry gas for extended time. Typical room temperature low pressure operation with unoptimized electrodes yielded 100 mA/cm² at 0.5V and maximum currents over 300 mA/cm² with low platinum loadings.

Our results clearly demonstrate that operation of proton exchange membrane fuel cells at ambient conditions is feasible. Optimization of the electrode-membrane structure is necessary to assess the full performance potential but we expect significant gains in weight and volume power density for the system. The reduced complexity will make fuel cells also attractive for smaller and portable power supplies and as replacement for batteries.

1.0 INTRODUCTION

Fuel cells are extremely attractive for extraterrestrial and terrestrial applications because of their high energy conversion efficiency (1). Among the various fuel cell systems the advanced polymer electrolyte membrane fuel cells based on sulfonated fluoropolymers (e.g., Nafion[®]) are relatively new but rapidly progressing. Proton exchange fluoropolymer membranes are particularly attractive because they are rugged, solid state, quite conductive, of good chemical and thermal stability and show good oxygen reduction kinetics due to their low specific adsorption on e.g., platinum catalysts. The proton exchange membrane fuel cell (PEMFC) exhibits its best performance at higher temperatures, e.g., 80°C and at elevated pressure, e.g., 5 atm of well humidified hydrogen and oxygen or air. These conditions result in minimum activation, ohmic and mass transport overpotentials even at current densities as high as 2 A/cm² (2). The gas conditioning and control functions necessary for optimum operation, are responsible for the fact that the cell stack is a vital but only small part of a complete power generating system. For larger fixed installations this approach appears to be advantageous to minimize cost. It precludes, however, the use of fuel cells for smaller and mobile applications. Here a near ambient temperature fuel cell which could operate satisfactorily without ancillary equipment for gas humidification and pressurization would be of great value and could replace batteries in many applications.

A large number of recent experimental and theoretical studies of PEMFC's and their components has contributed greatly to an advanced understanding of the systems operation and should lead to significant performance enhancement of practical units (3-11). These studies showed:

- Mass transport and resistance properties of PEM's are strongly dependent on the water content.
- The hydration level changes with temperature and environment (e.g., liquid H₂O, H₂O vapor).
- During current flow large hydration gradients are established across the membrane leading to commensurate inhomogeneities in membrane properties.
- Intimate catalyst ionomer contact and a high H₂O/SO₃H ratio are essential for efficient electrode reactions.
- Efficient electrode reactions are confined to very thin layers by ionic and mass transport resistances.

These findings show water management, electrode structure and electrode-membrane integration as the key parameters for a successful PEMFC. While basic studies try to separate the various processes to allow their investigation a practical device needs an optimal integration. We achieve this by precipitating the catalyst within the ionomer membrane. The resulting integrated catalyst-proton exchange polymer units have no interfacial barriers thus permitting unhindered water diffusion from cathode to anode. The results of our initial investigation are presented here.

2.0 PROJECT OBJECTIVE

The program objective is to demonstrate stable and attractive proton exchange polymer membrane fuel cell performance at near ambient temperatures without ancillary components for gas humidification or pressurization. Specific Phase I objectives included.

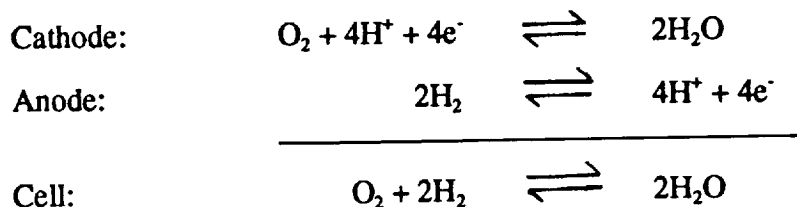
- Development of integral electrode-PEM components with the following characteristics:
 - Intimate catalyst ionomer contact
 - High catalyst utilization.
 - Low ohmic and mass transport resistances.
 - Tolerance to dimensional changes
- Cell performance demonstration with unhumidified H₂, O₂ and air at ambient temperature

3.0 PERFORMED RESEARCH AND DEVELOPMENT

3.1 Development of Integral Electrode-Membrane Units

3.1.1 General Background and Approach

The overall reaction in a hydrogen-oxygen fuel cell can be formulated as follows:



Thus 0.5 mole of water is generated per equivalent of charge. If the fuel cell is not operated in a dead ended mode some water is carried out with the exhaust gas stream (see Fig. 1). This is particularly significant if air is used as the oxidant.

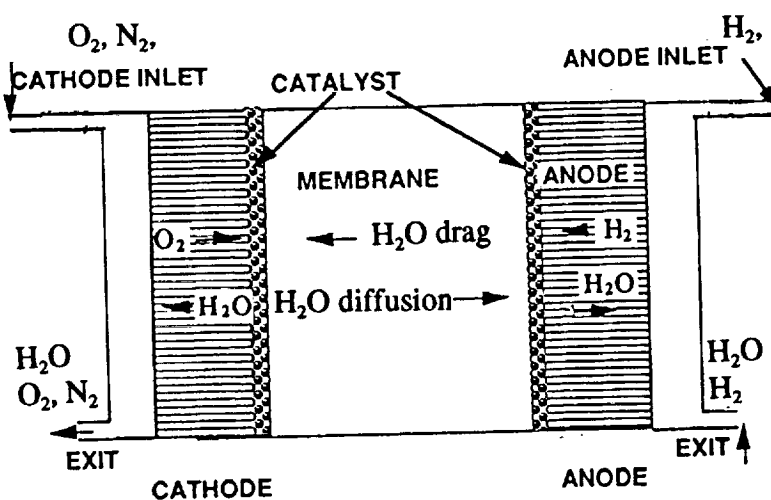


Fig. 1. Illustration of a solid polymer membrane fuel cell.

However, even here enough water is generated by the electrochemical reduction to compensate for the loss by evaporation up to 60°C at a flow rate corresponding to 50% oxygen depletion in the air stream. This mass balance is a necessary although not necessarily sufficient condition for stable operation. During current flow membrane water migrates with the protons from the anode to the cathode. Here additional reaction water is produced. This results in a tendency for the cathodes to flood while the anode and the membrane dry out. In fully hydrated Nafion® membranes ~4 H₂O are transported or dragged along with each proton (3). At lower water content in the membrane water transport decreases also. For Nafion® 117 drag coefficients for H₂O/H⁺ of 2.0 to 2.9 and 0.9 have been measured at 30°C for hydration levels of 22 and 11 H₂O/SO₃H, respectively (10). In an operating fuel cell concentration gradients in hydration level are established leading to water diffusion from the cathode to the anode. These opposing effects can result in little (12) or no (13) net water transport across the polymer membrane.

Water management appears also affected by the nature of the electrodes, in particular the cathode (14). A direct correlation is reported between the Teflon content and thus the hydrophobic character of the cathode and the net water transport showing a larger net water transport for a less hydrophobic electrode. This somewhat surprising finding may be connected with the equally surprising observation of Uribe et al. that reconstituted Nafion® membranes have different water content depending on whether they are in direct contact with liquid water or water saturated vapor (22 vs. 14 H₂O/SO₃H, (15)).

Water management in SPEFC's has generally been approached by operation with prehumidified gas streams often by saturation with water vapor at temperatures 5 to 15°C higher than the operating temperature of the fuel cell and by gas pressurization. In some studies the oxidant pressure exceeded the H₂ pressure (e.g., 5 atm vs. 3 atm) to further advance the driving force for water back diffusion (16).

What is needed for near ambient fuel cell operation without gas humidification are extremely thin, highly active electrodes in intimate contact with the ionomer to minimize hydration gradients. The cathode must generate and operate at high water content without flooding and the anode must function well at sufficiently low hydration level to achieve attractive cell performance without net water transport across the cell.

Our approach involves the controlled chemical-electrochemical reduction of a cationic platinum complex directly in the top surface of the ionomer. Wetproofed carbon structures in intimate contact with the catalyzed integral electrode-ionomer unit, but not actually bonded to it, serve both to prevent flooding of the cathode surface and as current collectors while providing easy access for the gaseous reactants.

3.1.2 Fabrication of Electrode-Membrane Structures

Test electrodes were prepared by the following procedures.

1. Reductive precipitation of unsupported platinum within the Nafion membrane.
2. Reductive precipitation of platinum on carbon black in the Nafion surface.
3. Bonding of conventional fuel cell electrodes to the Nafion membrane.

The commercially available proton exchange membrane Nafion[®] 117 (Dupont) was used throughout this investigation. The membrane was pretreated as follows: i) 3% H₂O₂ at 80°C, ii) 1N H₂SO₄ at 80°C, iii) boiling in doubly distilled water. The duration of each step was about one hour.

Platinum-Nafion Structures: Structures of dispersed platinum near the ionomer surface were prepared by chemical reduction of a cationic platinum complex which had been incorporated into the Nafion membrane via ion exchange (17,18). We used a solution of Pt(NH₃)₄Cl₂ which dissociates into the cationic Pt(NH₃)₄²⁺ and 2Cl⁻ ions. The reducing agent was NaBH₄. Specifically, the membrane was clamped in a masking fixture exposing only the 2 x 5 cm area to be catalyzed. This area was contacted with 10 cm³ of a 0.01M Pt(NH₃)₄Cl₂ solution for 30 minutes to allow for cation exchange. Then after a quick rinsing the membrane was immersed into 75 cm³ 0.08M NaBH₄ solution for 2 h. During this step the membrane turned gradually dark as platinum ions are reduced and the metal precipitates. Na⁺ ions enter the membrane to maintain charge balance. As a final step the catalyzed membrane was soaked in 1N H₂SO₄ at 80°C for 2 h to reconvert it into the protonated form followed by boiling in distilled water. For higher catalyst loadings we repeated the platinum precipitation sequence.

Carbon-Supported Platinum-Nafion Structures: Two types of electrode-membrane structures were prepared differing in the deposition of the carbon a) application of a carbon-Nafion solution slurry to the Nafion membrane followed by hot pressing and b) heat laminating a preformed carbon reconstituted Nafion layer) and the method of catalyzation a) electrodeposition from a H₂Pt(NO₂)₂SO₄ bath and b) chemical-electrochemical reduction of Pt(NH₃)₄Cl₂. Specific procedures were as follows:

For Type A structures a slurry containing 30 mg Vulcan XC72R carbon black (Cabot), 252 mg of a solution of 5% Nafion in alcohol and water/isopropanol to obtain a paintable consistency was ultrasonically mixed and painted onto an air dry Nafion membrane. After drying the membrane was placed between Teflon sheets, inserted into the heated press at 100°C, heated under light load to 125°C and then pressed at 80 atm for 90 s. The volume ratio of carbon/Nafion in the carbon was approximately 75%/25%. For platinum deposition the membrane structure was mounted into the plating fixture shown in Figure 2. A commercially available cationic platinum plating solution (platinum TP, 10g Pt/qt, Technic, Inc.) was used. Electrodeposition was carried out with a pulsed current regime of 10 mA/cm² for 30 s followed by 120 s rest. The total plating time was 30 min. Assuming the characteristic current yield for this bath of 1 Pt/15.5 e remains applicable. The 3.6 As/cm² are expected to result in a platinum loading of 0.5 mg/cm². After plating the catalyzed carbon-Nafion structure was soaked in 1N H₂SO₄ and H₂O at 80°C to remove foreign ions. An unsupported platinum electrode was deposited into the opposite side of the membrane using the procedure described earlier. For this, the electrode-membrane structure was clamped into a fixture similar to that shown in Figure 2 allowing only one side to contact the reducing agent.

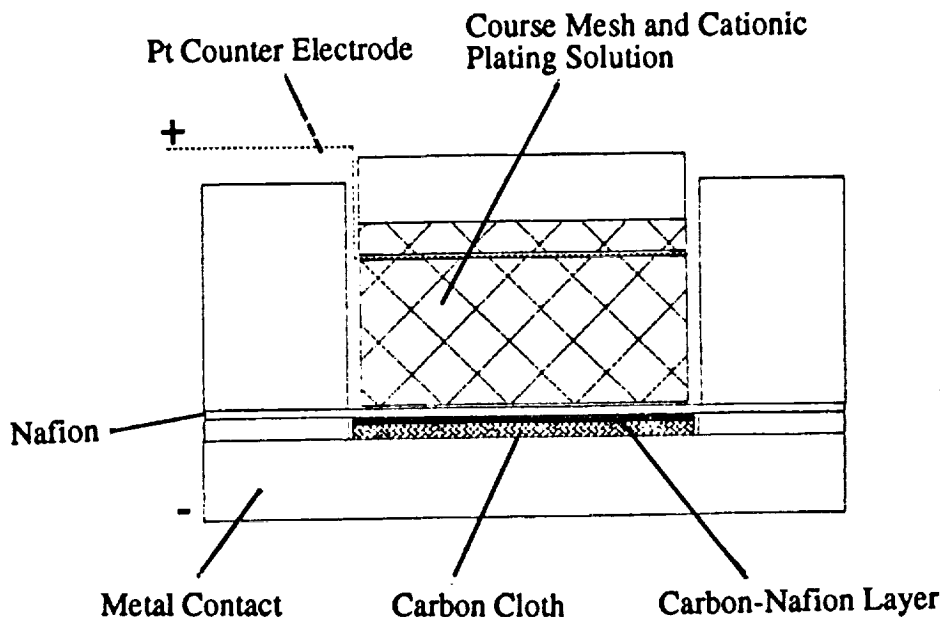


Figure 2. Illustration of platinum deposition by electroplating.

For Type B structures a Vulcan XC72R carbon black-Nafion solution slurry (composition as specified earlier) was painted onto a Kapton sheet, dried and cured at 135°C for 15 minutes. The resulting thin film was then laminated to the Nafion membrane by hot pressing using the regime described above. After cooling, the Kapton sheet was peeled off leaving a thin carbon-Nafion layer firmly bonded to the membrane. The carbon coated Nafion membrane was catalyzed by exchanging $\text{Pt}(\text{NH}_3)_4^{2+}$ into the membrane followed by reduction with NaBH_4 as described earlier.

Teflon-bonded Platinized Carbon-Nafion Structures: Electrodes consisting of Teflon bonded Vulcan XC-72 carbon black catalyzed with $0.35 \text{ mgPt}/\text{cm}^2$ on a carbon cloth substrate (E-Tek, Inc.) were modified by impregnation with Nafion. For this the active side of the electrode was brushed with a Nafion solution (5% Nafion in lower aliphatic alcohols and 10% water from Aldrich). The electrodes were air dried followed by vacuum drying at 70°C for 1.5 h. The Nafion membrane and the electrodes were bonded by hot pressing. The press was preheated to 110°C, the electrode-membrane assembly inserted under light load, the temperature raised to 120°C and then pressed at 60 atm for 1 minute.

3.1.3 Characterization of Electrode-Membrane Structures

Platinum-Nafion Structures: In the platinum-Nafion structures the catalyst is located close to the surface but within the Nafion membrane. Scanning electron micrographs of cross sections obtained by fracture under liquid N_2 indicate a layer thickness of about $1 \mu\text{m}$ (Fig. 3). The interior border is diffuse and a decreasing density of platinum particles can be seen to a depth of about $2 \mu\text{m}$. This is particularly evident in the back scatter picture of Figure 4. The surface has a metallic appearance with small cracks which may however result from sample drying during evacuation

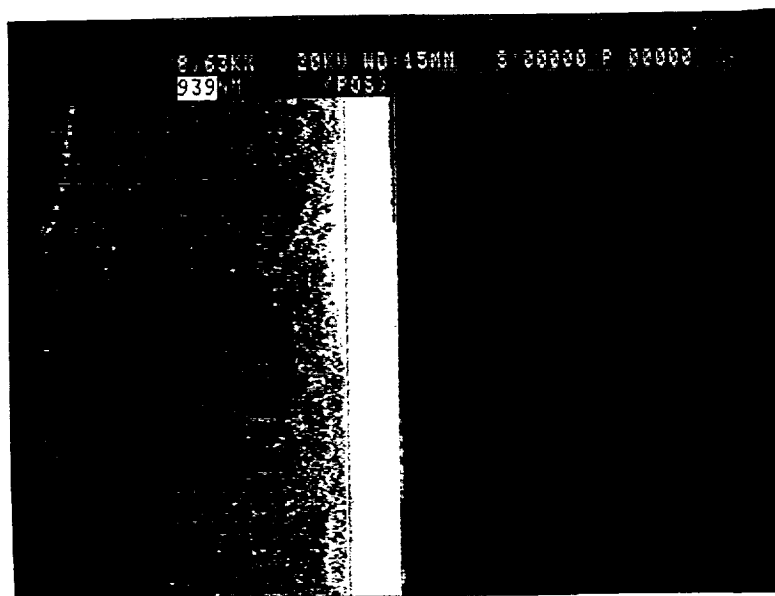


Figure 3. Cross-section of an integral Nafion-platinum electrode unit after two impregnation-reduction steps.

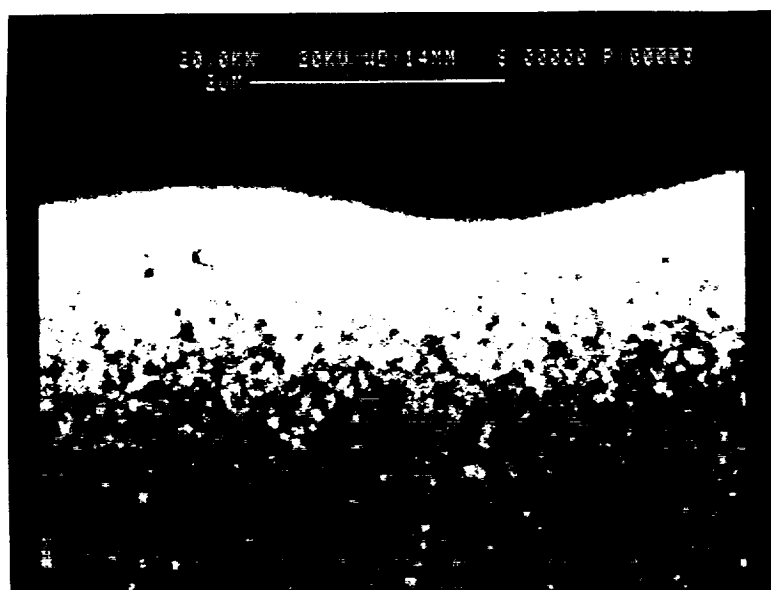


Figure 4. Scanning electron micrograph (back scatter mode) showing the cross-section of an integral Nafion-platinum electrode unit after two impregnation-reduction steps.

(Fig. 5). Surface resistance measurements indicated good electrical contact and lateral conductance. There was no electronic path between the electrodes across the membrane. The platinum loading was approximately 1.9 mg/cm^2 . The value was determined gravimetrically after completely oxidizing the organic components by heating in air to 850°C . This loading would correspond to an average 60% volume occupation in the $1.5 \mu\text{m}$ surface layer with a higher metal fraction close to the surface and a lower one towards the interior.

The electrochemically accessible platinum surface area of the electrode was determined via the hydrogen adsorption charge obtained from a cyclic voltammogram during an inert gas purge after correction for double layer charging (Fig. 6). Assuming $Q_{\text{H}_2} = 0.21 \text{ mCoul/cm}^2$ we calculated a Pt roughness factor of about 93.

Carbon Supported Platinum-Nafion Structures: The macroscopic and microscopic surface morphology of a Type A platinum catalyzed carbon-Nafion structure is shown in Figure 7. A cross section obtained by fracturing under liquid nitrogen is shown in Figure 8. The carbon-reconstituted Nafion layer was with $15 \mu\text{m}$, relatively thick. Elemental analysis by EDAX showed platinum in the carbon-layer (Fig. 9) and in the Nafion at the carbon-Nafion interface. The latter is also visible in the back scatter picture shown in Figure 8. About $10 \mu\text{m}$ into the Nafion membrane (at the location of the dark burn hole in Fig. 8) only F and S from the membrane but no platinum was detected (Fig. 10). The cyclic voltammogram used to determine the charge for hydrogen adsorption is shown in Figure 11. The electrochemically accessible platinum surface area was very low resulting in a roughness factor of only 12. Apparently the platinum plating efficiency was considerably lower than expected.

The surface morphology and cross section of a carbon supported platinum-Nafion structure of Type B are shown in Figures 12 and 13, respectively. The Nafion bonded carbon layer was with $\sim 10 \mu\text{m}$ relatively thick. Platinum, identified by energy dispersive X-ray analysis, was found in the Nafion-carbon layer and in the adjacent Nafion membrane. Elemental mapping showed a considerable concentration of platinum at the Nafion membrane-carbon layer interface (Fig. 14). The platinum area in contact with the electrolyte was again determined from the charge of adsorbed hydrogen obtained from the cyclic voltammogram (Fig. 15) after correction for the double layer capacity. It yielded a platinum roughness factor of 37. We measured a very low platinum loading of 0.05 mg/cm^2 . This result may, however, underestimate the actual loading since some crucible attack occurred in the experiment.

3.2 Fuel Cell Performance Evaluation

3.2.1 Experimental Conditions

Test Cell: Two test cells were used. They are illustrated in Figures 16 and 17. The active electrode area was 10 cm^2 ($2 \text{ cm} \times 5 \text{ cm}$). Electrical contact and gas distribution was achieved with a woven carbon cloth (PWB-6, Zoltek Corp.). As current collector plate we used stainless steel which was later gold plated to reduce the contact resistance. The cell shown in Figure 17 is of similar construction except that it allowed to vary the compression of the electrode-carbon backing assembly without affecting the cell seal.

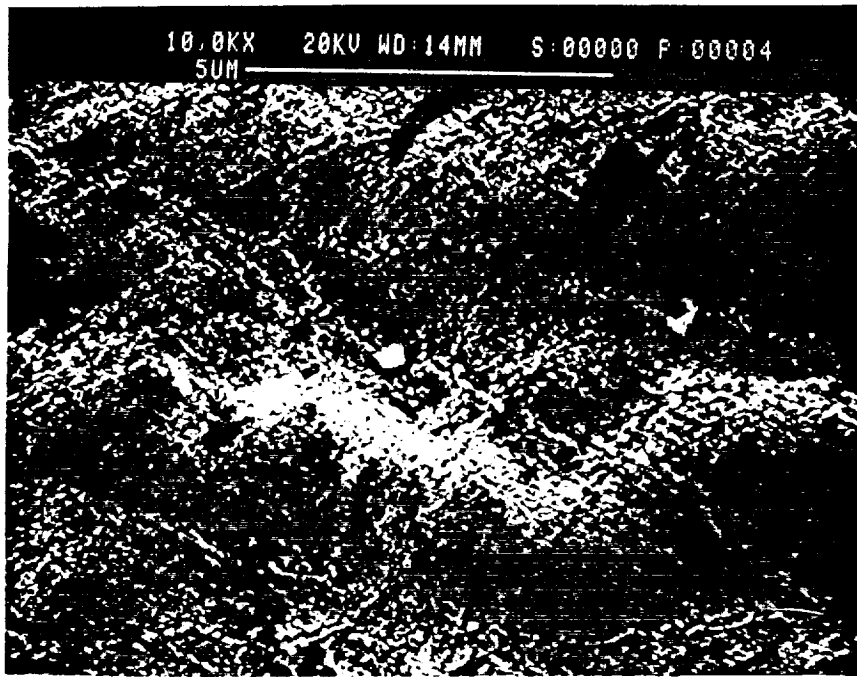


Figure 5. Scanning electron micrograph showing the surface of an integral Nafion-platinum electrode unit after two impregnation-reduction steps.

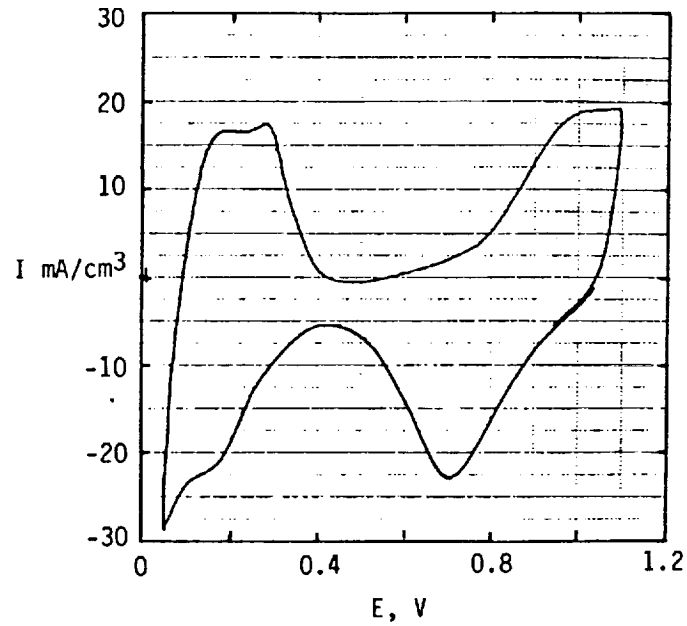


Figure 6. Cyclic voltammogram of an integral platinum-Nafion membrane fuel cell electrode. Two impregnations. Sweep rate = 20 mV/s.

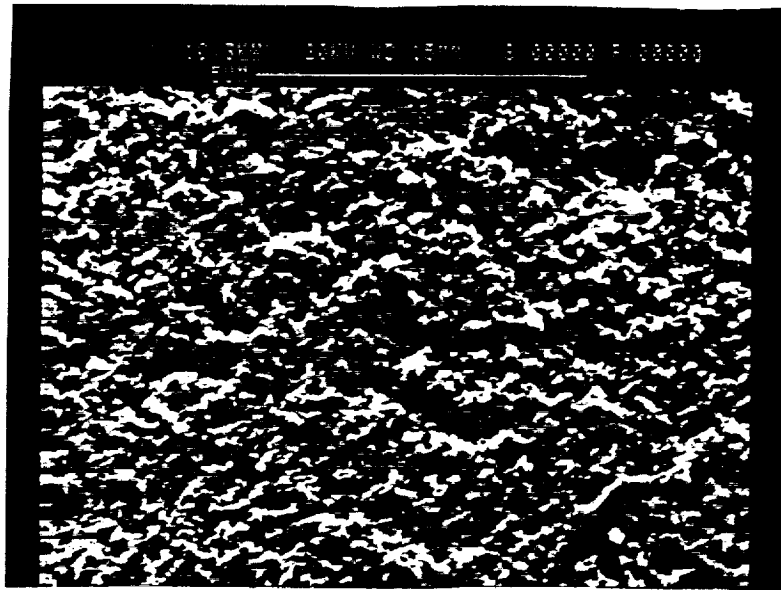
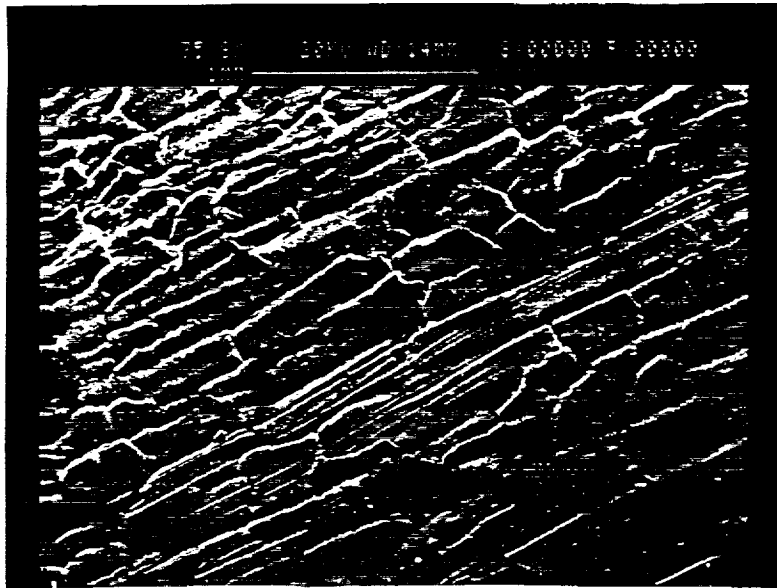


Figure 7. Surface of a carbon supported platinum-Nafion structure (Type A).

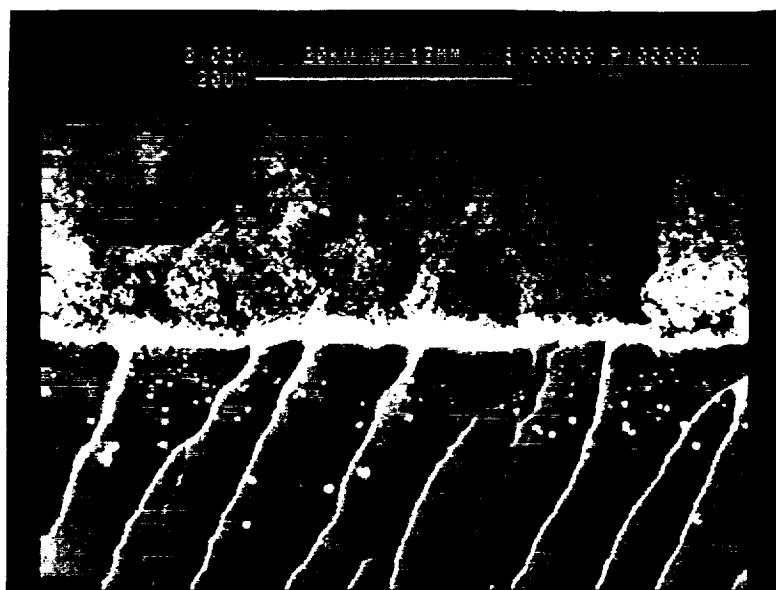
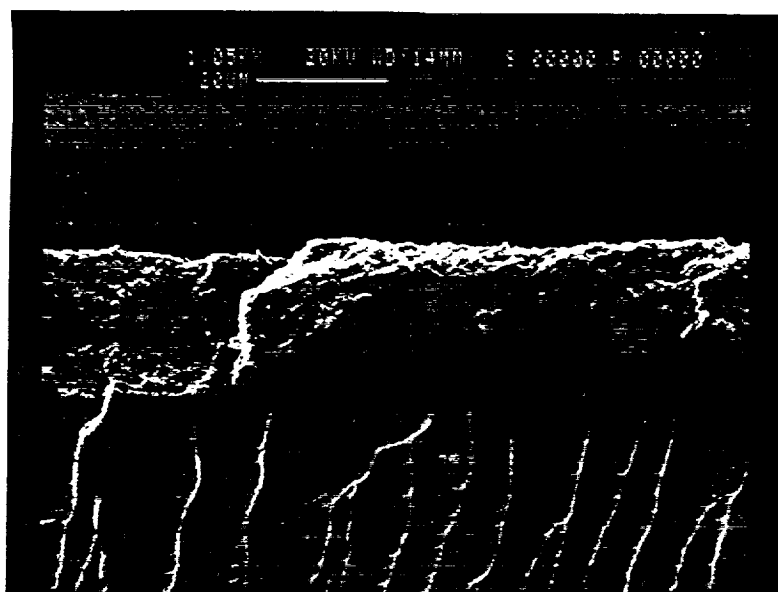


Figure 8. Cross section of a carbon supported platinum-Nafion structure (Type A). Upper picture, secondary electron image 35° angle; lower picture, back scatter image.

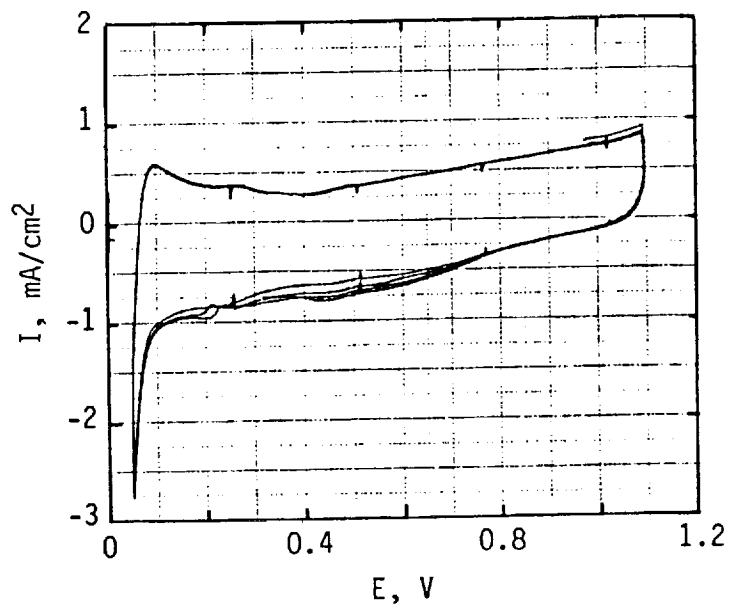


Figure 11. Cyclic voltammogram of an integral platinized carbon-Nafion (Type A). Sweep rate = 20 mV/s.

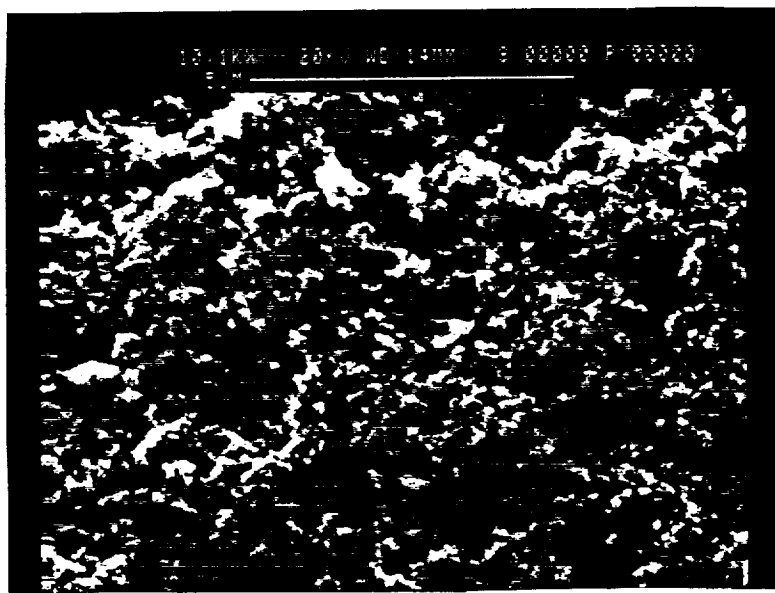


Figure 12. Scanning electron micrograph showing the surface of an integral platinized carbon electrode-Nafion structure.

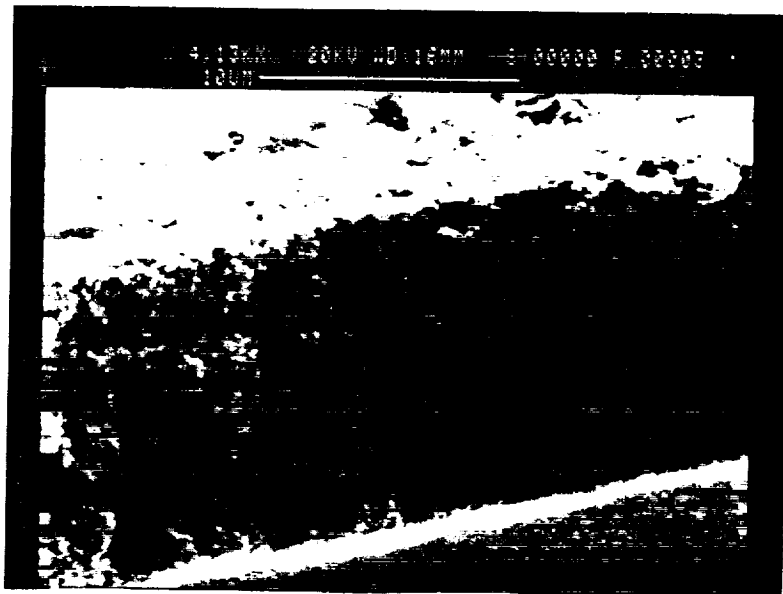


Figure 13. Cross-section of an integral platinized carbon electrode-Nafion structure.

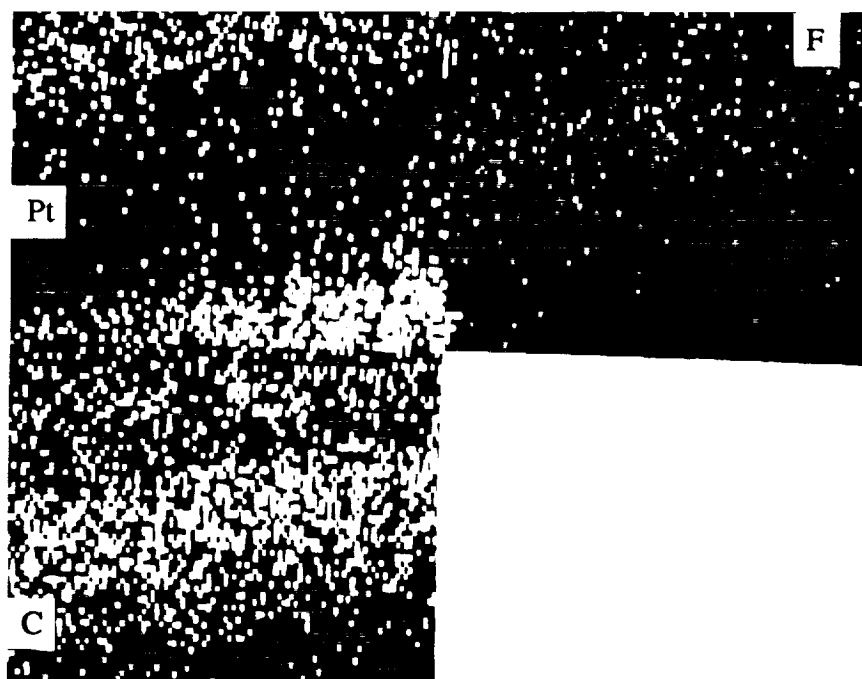


Figure 14. Elemental intensity for Pt, C and F of the electrode-membrane cross section shown in Fig. 13.

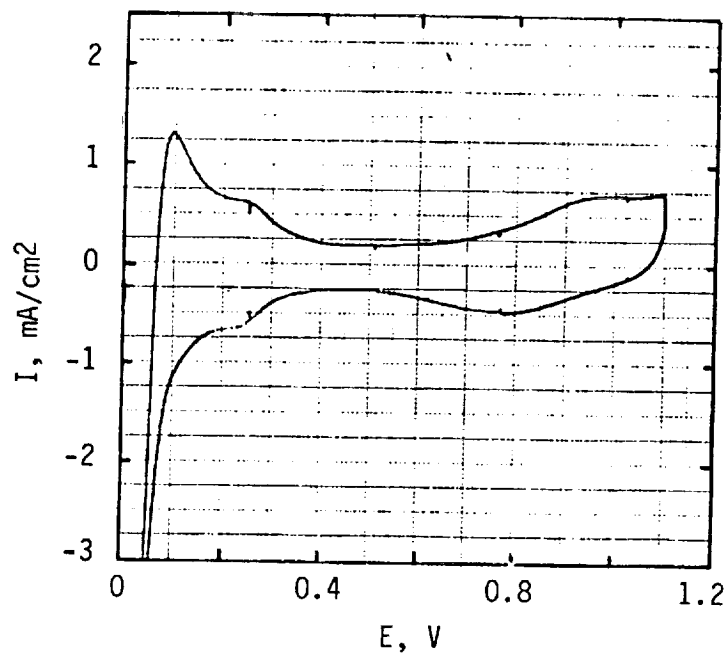


Figure 15. Cyclic voltammogram of an integral platinized carbon-Nafion structure (Type B). Sweep rate = 20 mV/s.

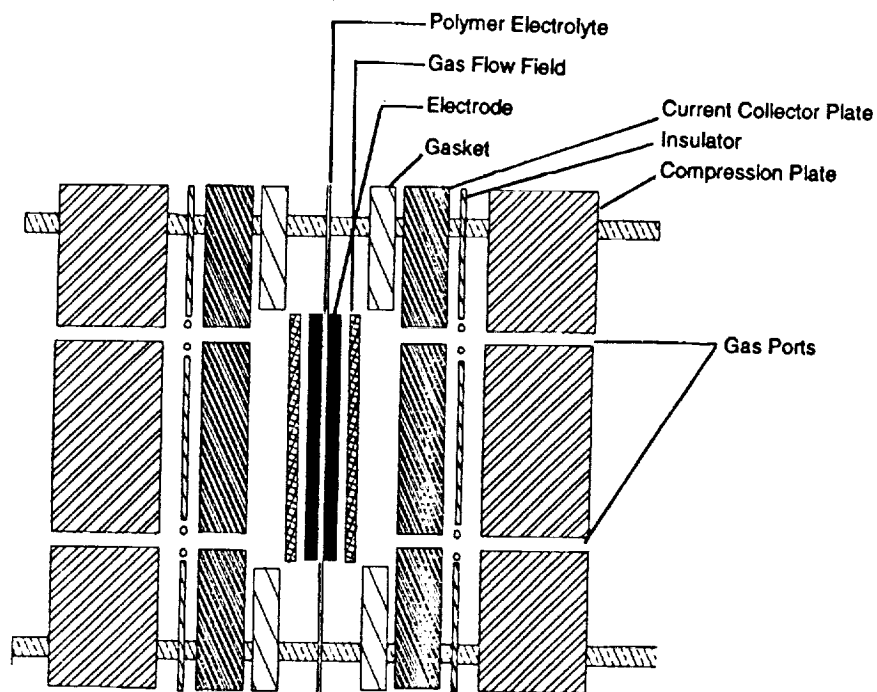


Figure 16. Illustration of the test cell (exploded view).

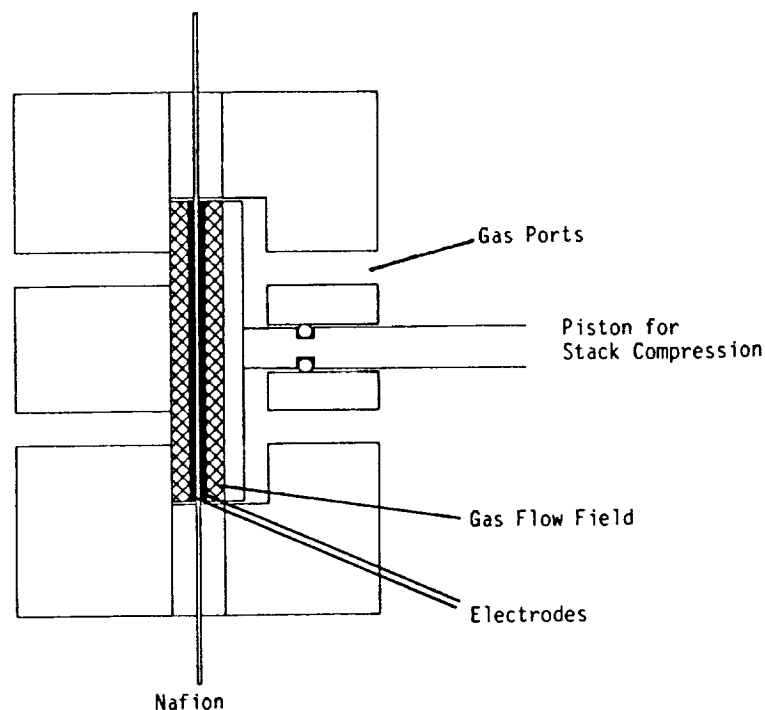


Figure 17. Illustration of the test cell allowing variation of cell stack compression.

Test Station: The fuel cell test station is schematically shown in Figure 18. The flow of hydrogen, oxygen and air was measured and controlled by mass flow controllers (Tylon General). Nitrogen could be flushed through the anode compartment during start up and shut down. A controlled galvanostatic or potentiostatic load could be applied to the cell. Current and voltage were recorded on a multichannel data acquisition system (Bascom-Turner 8000). In addition, we used a current interrupter (ESC, 800 IR measuring system) to measure the ohmic voltage drop through the Nafion membrane and cell contact resistances. A Teflon bonded platinum electrode, attached external to the cell to the protruding Nafion membrane and exposed to air, was used as a relative reference electrode. Hydrogen (grade 4.7), oxygen (grade 2.6) and air (dry) were obtained as compressed gases from Airco. All experiments were conducted with dry gases between 1 and 2 atm and at temperatures of 10° to 50°C. Prior to the measurement of current-potential curves the cell was run under load to allow for membrane hydration and cell equilibration. H₂ and O₂ were generally used at small bleed rates while air flow was adjusted to consume less than half the oxygen.

3.2.2 Fuel Cell Test Results

3.2.2.1 Teflon Bonded Electrode-Membrane Assemblies

The behavior of fuel cell assemblies with unmodified and Nafion solution modified Teflon bonded electrodes operating on dry gases at ambient temperatures was determined as base line. Measurements performed between 11°C and 50°C yielded very similar results. A typical potential-current plot is shown in Figure 19. Selected performance values are compared in Table 1. At lower temperatures the reduced electrode kinetics and ion mobility appears to be nearly compensated by the increased gas solubility in the electrolyte. Both electrodes showed considerable

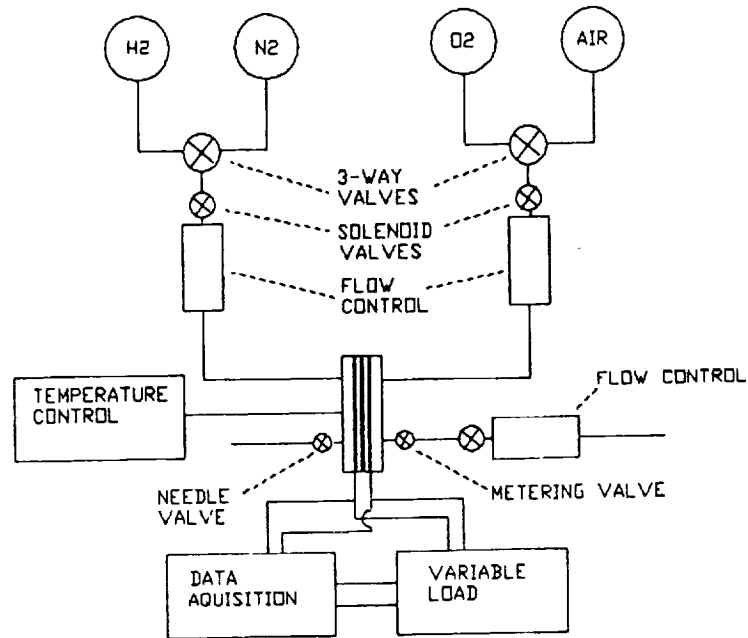


Figure 18. Schematic illustration of the fuel cell test station.

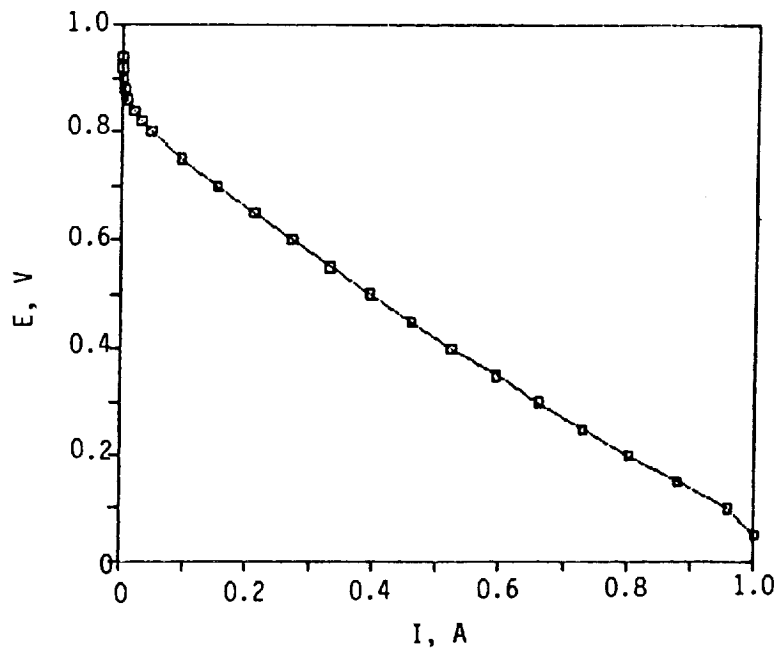


Figure 19. Potential-current plot for fuel cell I. 30°C, 2.0 atm H₂ and O₂.

Table 1. Test Summary of Fuel Cell Assembly No. 1.*

Test No.	T (°C)	P _{gas} (atm)		E _{iso} (V)	I _{E=0.4} (mA)	η _{H₂} (mV)	η _{O₂} (mV)	R (Ω)
		H ₂	O ₂					
1	50	1.3	1.3	0.940	375	-	-	0.28
2	50	2.0	2.0	0.957	490	247	310	0.31
3	30	2.0	2.0	0.940	510	200	340	0.44
4	20	2.0	2.0	0.950	465	210	340	0.35
5	11	2.0	2.0	0.963	391	231	330	0.37
6	50	1.7	2.0	0.967	611	149	418	0.28
7	50	1.3	1.3 ¹⁾	0.908	232	244	264	0.51
8 ²⁾	50	2.0	2.0	0.980	853	54	526	0.16
9 ³⁾	50	1.3	1.3	0.940	643	141	399	0.32

*Nafion impregnated cathode, unmodified E-Tek anode.

¹⁾Air.

²⁾Anode and cathode exchanged.

³⁾Cell with adjustable stack compression.

polarization. Normally the cathode polarizes predominantly. Here the anode polarization reflects the lower activity of the unmodified anode and the reduced hydration level of the Nafion membrane at the anode side. The effect of electrode modification is clearly illustrated by run 8 where the anode and cathode were reversed. This resulted in low anode and high cathode polarization. The resistances measured by current interruption were 5 to 10 times higher than what one would expect from a fully hydrated Nafion membrane. A major part of this resistance appeared to result from interface contacts between the electrodes and the current collectors in the experimental cell. To gain better control of this component we modified the test cell as shown in Figure 17. A movable piston was introduced which allowed variation of the electrode stack compression without affecting the gas seal of the cell.

The critical effect of membrane hydration is illustrated in Figure 20 which shows the current and cell resistance at a constant cell potential of 0.5V. After operating at a stable current for 16 h the O_2 flow rate was increased from 5 cm^2/min to 100 cm^3/min . This resulted in membrane drying leading to complete current cutoff and a substantial resistance increase. After closing the gas bleed, the cell began to recover. This recovery accelerated as the reactant water rehydrated the membrane. The cell resistance showed a commensurate decrease reaching the original value. The current did not fully recover to its original value until the cell was temporarily operated at lower voltage (0.1V, 930 mA). The higher rate of water generation apparently promoted enhanced membrane hydration. This is consistent with observations by the research groups at the Los Alamos National Laboratory regarding the hydration level of Nafion as a function of the mode of water supply (6). Upon reaching the full current of 335 mA at time 415 min the charge of 686 As has generated 64 mg H_2O of which about 14 mg may have been removed by the bleed gas stream. The remaining 50 mg of water would correspond to about 9 to 10 H_2O/SO_3H as a membrane average. This is in good agreement with the water content reported for Nafion 117 membranes of 14 H_2O/SO_3H and 7 H_2O/SO_3H at water activities of 1.0 and 0.8, respectively. We demonstrated also stable extended time operation of the fuel cell on unhumidified gases. An example is shown in Figure 21.

Improved cell performance was obtained with fuel cell assembly No. 2 in which the anode and cathode consisted of Nafion modified E-Tek fuel cell electrodes (~ 0.1 and 0.2 mg Nafion/ cm^2 for the anode and cathode, respectively) and which contained a more efficient current collector. A typical current-potential relationship is shown in Figure 22. Additional results are shown in Table 2. Reversal of the electrode assembly showed again that the original cathode was the more electrocatalytically active electrode. Careful optimization of the electrode-membrane interface is essential for good cell performance especially at ambient temperature and without gas humidification.

3.2.2.2 Platinum-Nafion Structures

The integral membrane-electrode unit was mounted into the test cell with a woven carbon cloth and a Teflon bonded carbon electrode as anode and cathode collectors, respectively. Tests were performed over a wide range of conditions. Characteristic current potential curves for oxygen and air at 2.0 and 1.3 atm are shown in Figures 23 through 26. The cell operating at 20°C on unhumidified hydrogen and oxygen delivered 1A (100 mA/ cm^2) at 0.5V. At low currents the polarization results almost entirely from the cathode. At higher currents the anode polarization

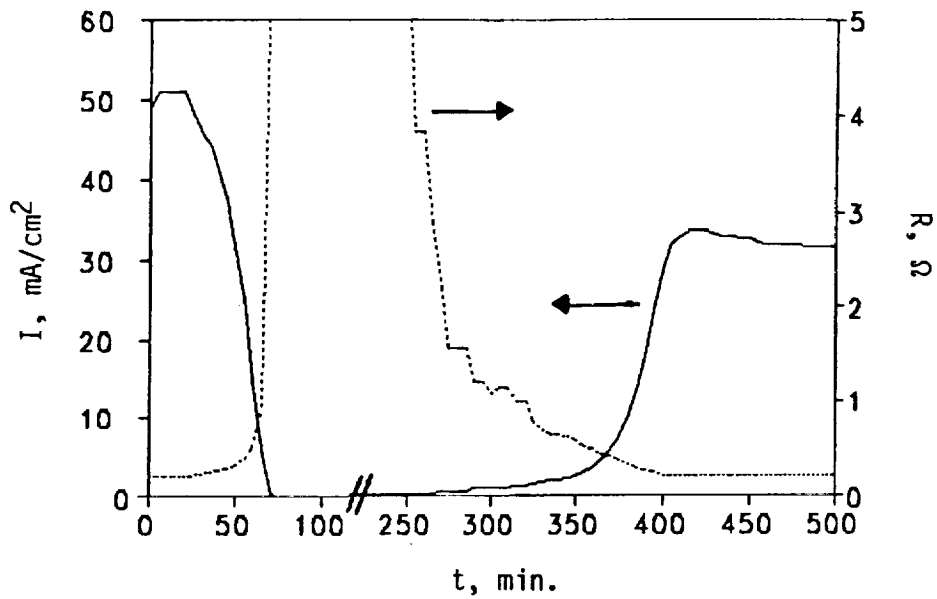


Figure 20. Current changes at a constant cell potential of 0.5V as a function of dehydration and rehydration of the Nafion membrane. 50°C, 1.3 atm H₂, 1.3 atm O₂, O₂ purge rates: 0 to 220 min; 100 cm³/min; 220 to 385 min; 0 cm³/min; 385 to 500 min; 5 cm³/min. Cell resistance measured by current interruption.

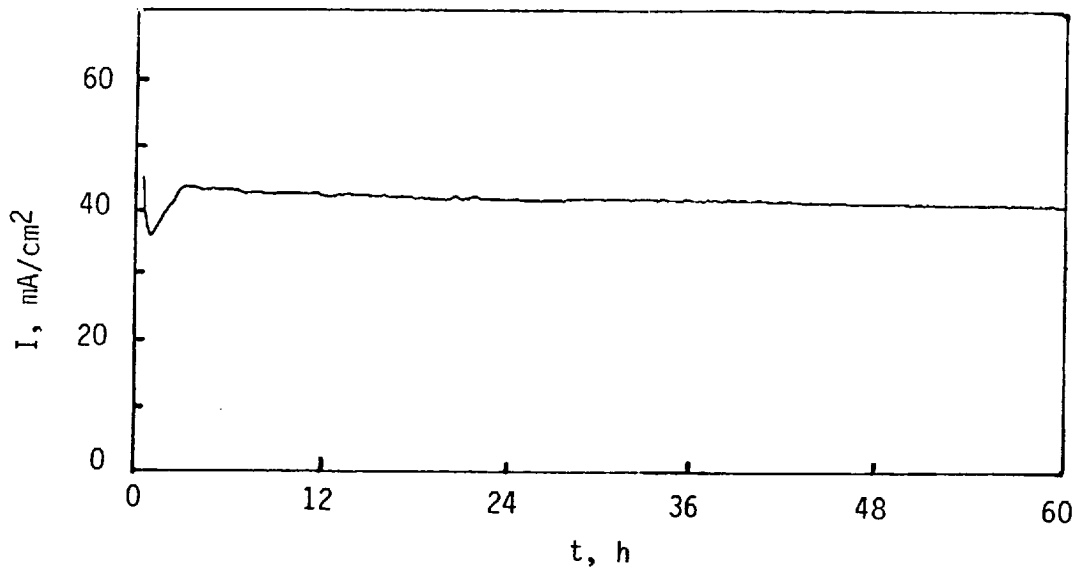


Figure 21. Extended fuel cell operation at 0.5V without gas humidification 30°C 1.3 atm H₂, 1.3 atm O₂, O₂ purge 5 cm³/min.

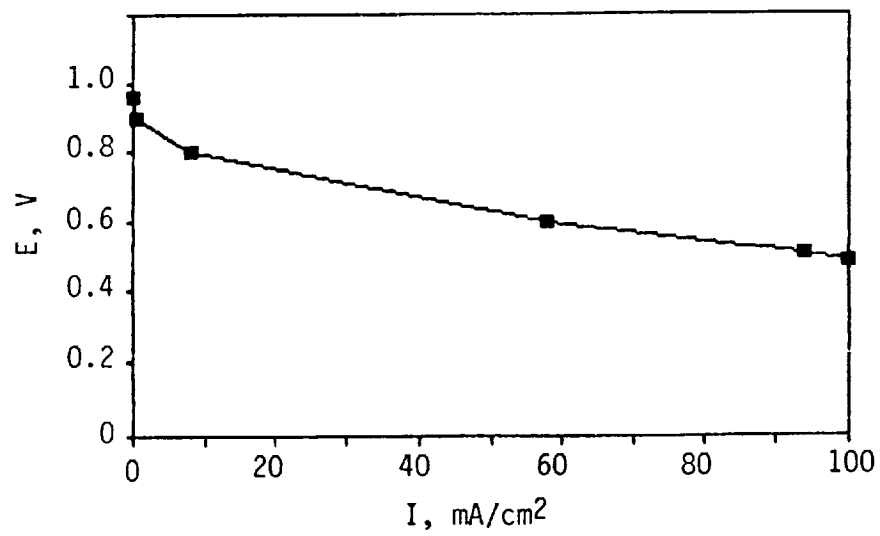


Figure 22. Potential-current plot for fuel cell II. 50°C, 1.3 atm H₂ and O₂.

Table 2. Test Summary of Fuel Cell Assembly No. 2.*

Test No.	T (°C)	P _{g^m} (atm)		E _{t=0} (V)	I _{E=0.5} (mA)	η _{H₂} (mV)	η _{O₂} (mV)	R(Ω)	
		H ₂	O ₂						
1	50	1.3	1.3	0.990	325	213	269	-	
2	50	1.3	1.3	0.950	515	-	-	Improved current collector.	
3	50	1.3	1.3	0.965	940	-	-	0.15	
4	20	1.3	1.3	0.948	810	228	220	0.12	
5	20	1.3	1.3	0.945	840	55	390	0.13	
									Anode and cathode exchanged.

*Nafion modified E-Tek electrodes.

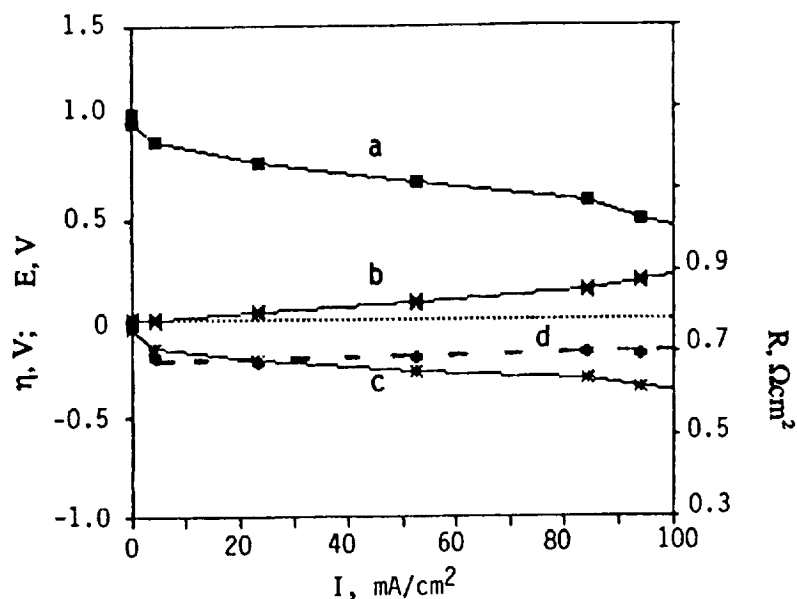


Figure 23. Potential-current behavior of a fuel cell with integral Nafion-platinum electrodes operating at 20°C on unhumidified gas. 2 atm H_2 and O_2 ; a = cell voltage, b = anode polarization, c = cathode polarization and d = cell resistance.

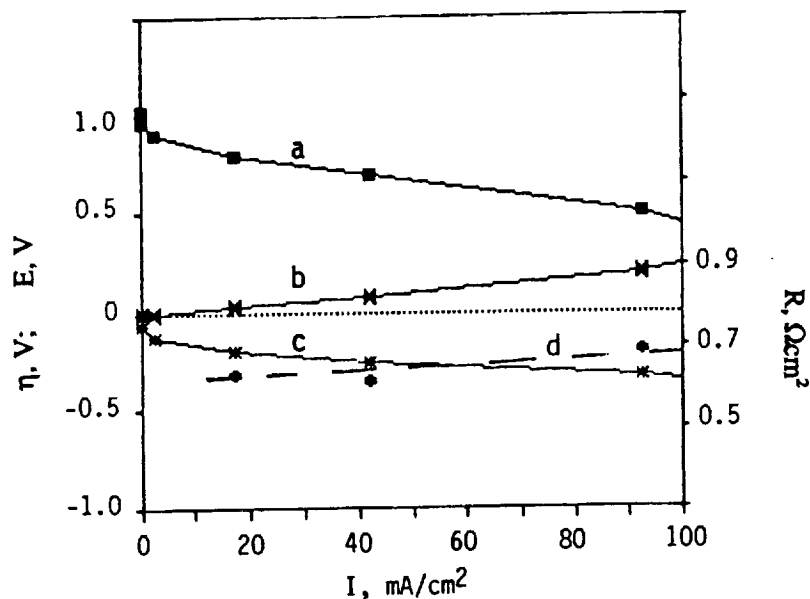


Figure 24. Potential-current behavior of a fuel cell with integral Nafion-platinum electrodes operating at 20°C on unhumidified gas. 1.3 atm H_2 and O_2 ; a = cell voltage, b = anode polarization, c = cathode polarization and d = cell resistance.

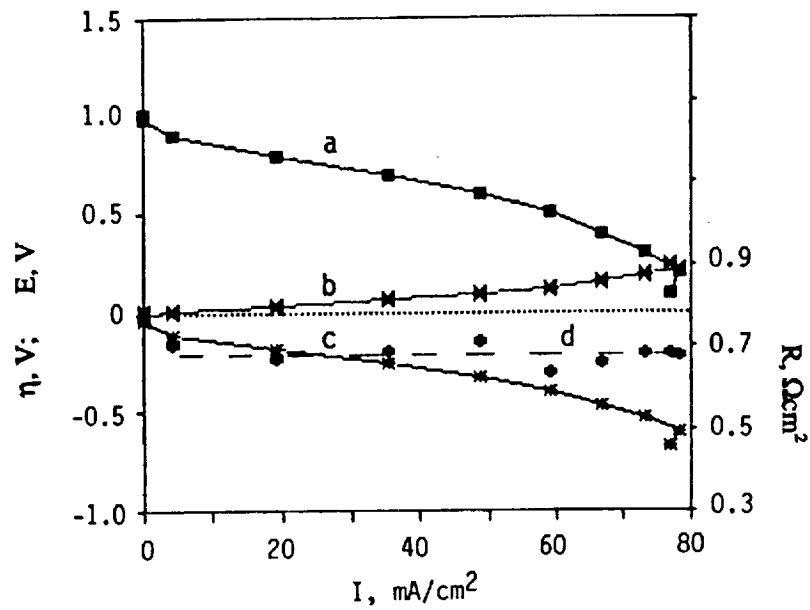


Figure 25. Potential-current behavior of a fuel cell with integral Nafion-platinum electrodes operating at 20°C on unhumidified gas. 2 atm H_2 and air (airflow 60 $\text{cm}^3/\text{min}.$); a = cell voltage, b = anode polarization, c = cathode polarization and d = cell resistance.

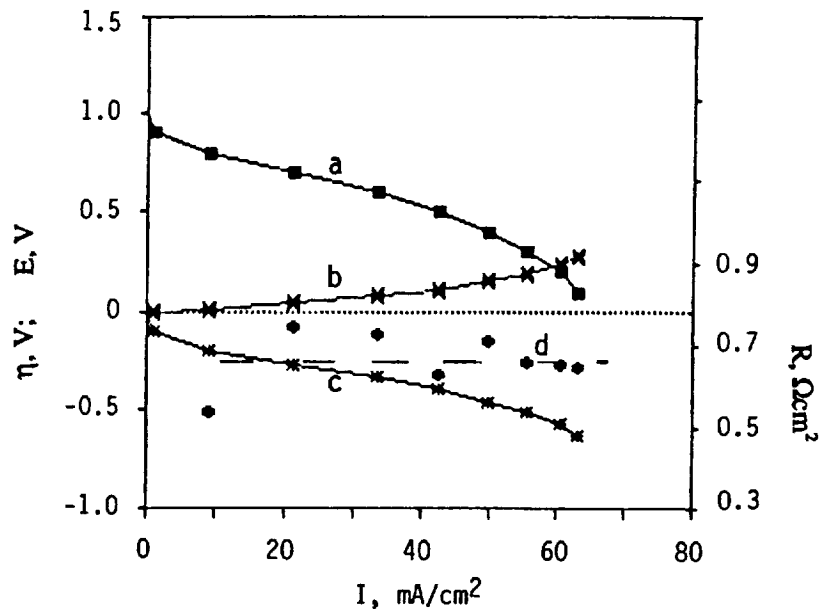


Figure 26. Potential-current behavior of a fuel cell with integral Nafion-platinum electrodes operating at 20°C on unhumidified gas. 1.3 atm H_2 and air (airflow 60 $\text{cm}^3/\text{min}.$); a = cell voltage, b = anode polarization, c = cathode polarization and d = cell resistance.

increased and at 100 mA/cm² it contributed almost 40% towards the total cell polarization. The cell resistance, measured by brief current interruption, showed only a very slight increase. It reflected the resistance across the membrane and any electronic contact resistance in the test cell but excluded components within the porous electrodes. The change in oxygen pressure between 1 and 2 atm had only a small effect on the current-potential behavior. The change from oxygen to air is, however, quite significant. In addition to an expected increase in the cathode polarization we observed also a smaller but noticeable increase in the anode polarization. The most likely reason is a lower water saturation at the cathode due to the higher gas bleed rate which is necessary for operation with air. An analysis of the oxygen gain, which is the voltage difference of the cathode between operation on air and oxygen at a fixed current density, indicates an electrode performance limitation beyond activation control and diffusion in the electrolyte adjacent to the catalyst emphasizing the need for the optimization of the electrode structure.

The dehydration and subsequent rehydration of the membrane is illustrated in Figures 27 and 28. At high purge rates with unhumidified gas, especially at elevated temperatures, the Nafion membrane can lose sufficient water to completely cut off current flow. Membrane resistance assumes values beyond 100 Ωcm². It is worth noting that, during potentiostatic operation, the cell current declines substantially long before a significant increase in membrane resistance was measured. Obviously the effect of low hydration on the electrode reactions is the critical factor rather than the increase in membrane resistance. Both electrodes were affected. Initially, the anode polarization increased slightly as the current started to decrease followed by a gradual decrease to about 30 mV at currents below 40 mA. The main polarization occurred at the cathode.

Rehydration of the membrane proceeded initially very slowly and then accelerated as the current increased and with it the generation of reaction water at the cathode. For the example shown in Figure 28, the incorporation of 1 H₂O/SO₃H, which occurred at approximately 26 min., lowered the membrane resistance to 5 Ωcm². With the current of 15 mA/cm² this yields an ohmic potential drop of 75 mV. While not insignificant it is only about 15% of the total cell polarization.

A steady state current was reached at 60 min. after generation of 4.57·10⁻⁴ mole H₂O. This would correspond to an average membrane hydration level of 14.7 H₂O/SO₃H, or after adjustment for 0.4 to 0.5 H₂O/SO₃H, removed with the oxygen bleed stream to slightly above 14 H₂O/SO₃H. These findings are in excellent agreement with hydration levels recently reported by the research group at Los Alamos National Laboratory (6).

The individual electrode potentials, measured against a cell external air reference electrode, did not change much during the rehydration run. A small (~40 mV) minimum in cathode polarization and a corresponding maximum in anode polarization was observed at about half the final current. The cell was run potentiostatically for 16 h delivering a nearly constant current.

3.2.2.3 Carbon Supported Platinum-Nafion Structures

The integral electrode-membrane units were mounted into the test cell as described earlier using a Teflon bonded carbon electrode and a carbon cloth as the cathode and anode current collectors, respectively. The potential-current behavior for an A type electrode-membrane structure

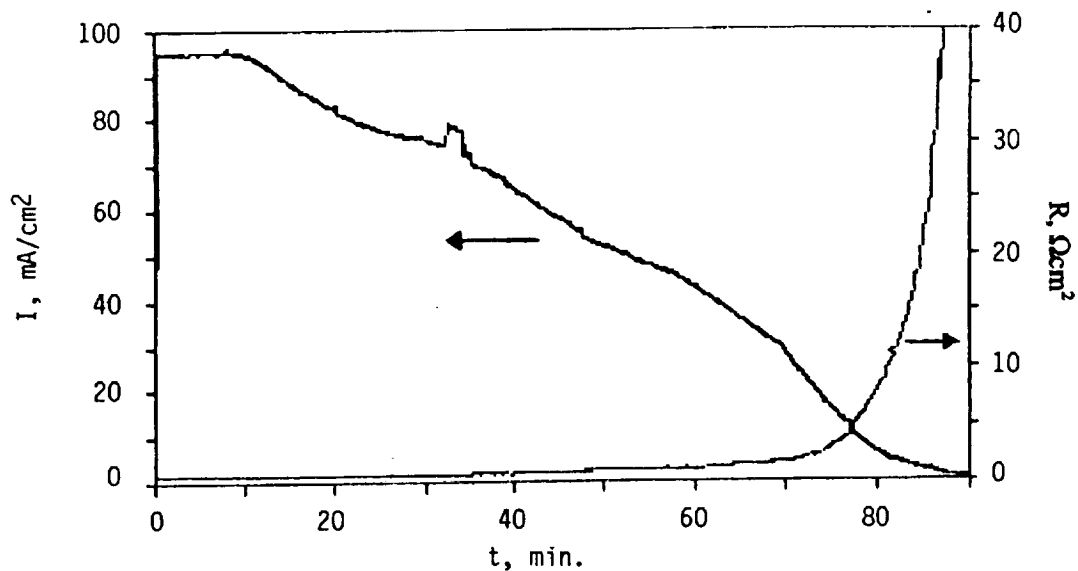


Figure 27. Current and membrane resistance during platinum dehydration of an integral Nafion-electrode unit upon potentiostatic fuel cell operation on unhumidified gas. Cell voltage 0.55V; $T = 50^{\circ}\text{C}$; 1.3 atm H_2 without bleed; 1.3 atm O_2 ; 120 cm³/min. bleed.

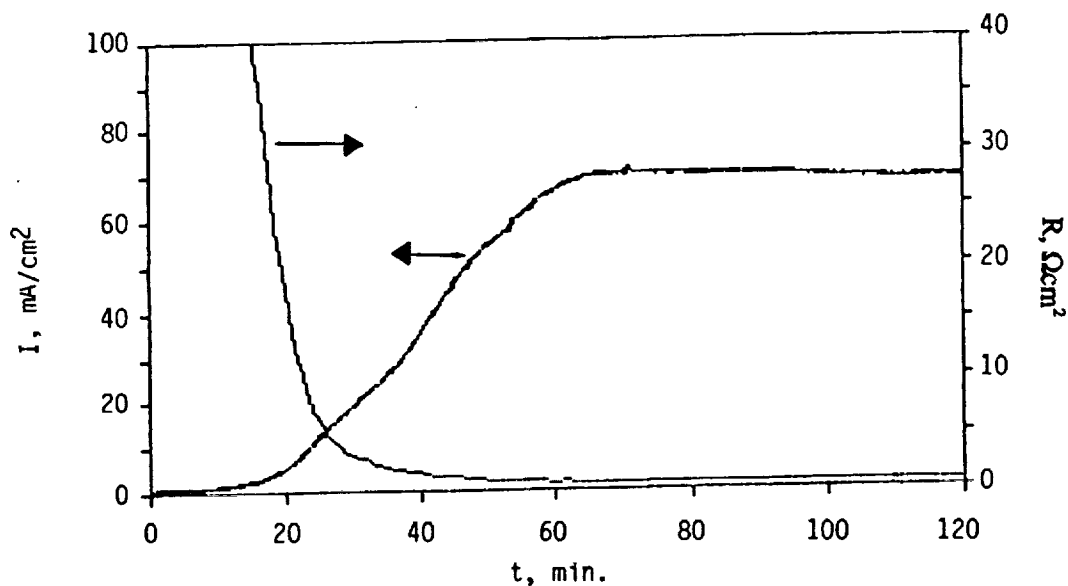


Figure 28. Current and membrane resistance during self hydration of an integral Nafion-platinum electrode unit upon potentiostatic fuel cell operation. Cell voltage 0.55V; $T = 20^{\circ}\text{C}$; 1.3 atm H_2 ; 1.3 atm O_2 ; gas bleed 7 cm³/min. at $t > 30$ min.

at room temperature and 1.3 atm reactant pressure is shown in Figure 29. The cell showed significant polarization originating almost exclusively from the cathode. This is not surprising in view of the very low platinum loading of this electrode resulting in a roughness factor of only 12. It is worth noting that reactant transport appears not to be limiting within the range of the test. The performance of a Type B electrode-membrane structure at 20°C and 50°C are shown in Figures 30-32. Similar performance was observed at both temperatures with currents over 300 mA/cm². At lower currents the cell polarized less at the higher temperature as might be expected. In this region a larger fraction of the overall polarization resulted from activation polarization at the cathode which had only a moderate platinum roughness factor of 37. The high cell polarization shown in Figure 32 is the result of cathode flooding. To illustrate the importance of the current collector component in regulating the water removal and gas access, this cell was assembled with a non wetproofed carbon cloth contact component. There was no indication of large reactant transport limitations below 300 mA/cm² in this electrode despite the unfavorable catalyst distribution which places the bulk of the platinum quite far removed from the electrode surface.

Figures 33 and 34 show the change in current and ohmic resistance of the electrode-membrane structure at constant potential during dehydration at 50°C and self rehydration at 20°C. The cell current started to decrease soon after the oxygen flow had been increased. The membrane resistance increased noticeably only much later after the current had decreased to about 25% of the original value. After dehydration at 50°C the cell was cooled to 20°C and the gas bleed was stopped. The self rehydration of the cell is shown in Figure 34. The initial recovery was slow but accelerated as reaction water was produced. After 75 min. the oxygen bleed was set at 10 cm³/min. to avoid the accumulation of inert gas in the cathode compartment. The current reached a maximum followed by a slow gradual decline to about 0.5A after 16 h which was close to the value previously measured during the current-potential studies. The most likely cause for this current decline is a partial flooding of the cathode which can be avoided by an appropriate electrode structure.

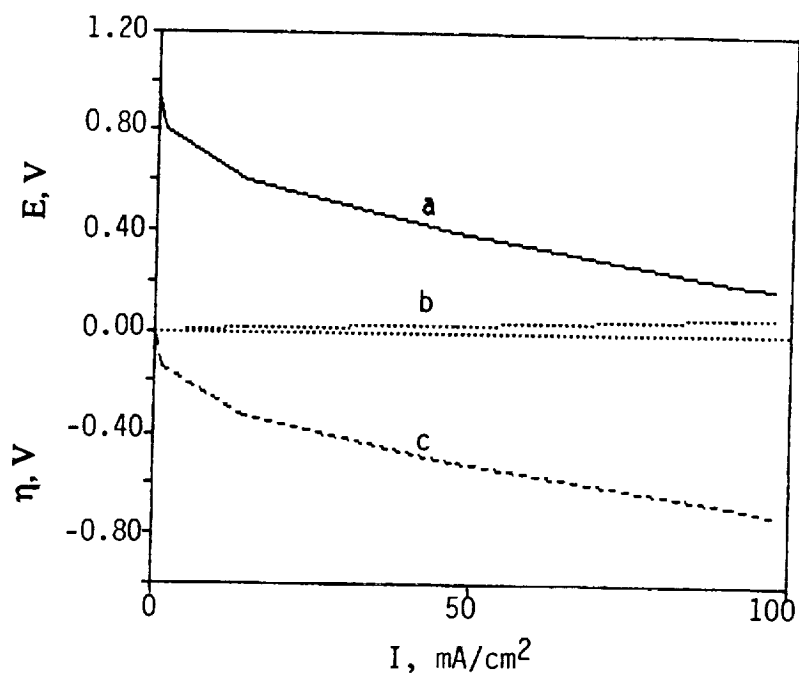


Figure 29. Current voltage behavior of a carbon supported platinum-Nafion structure (Type A). 20°C, 1.3 atm H₂ and O₂. a, cell voltage; b, anode polarization and c, cathode polarization.

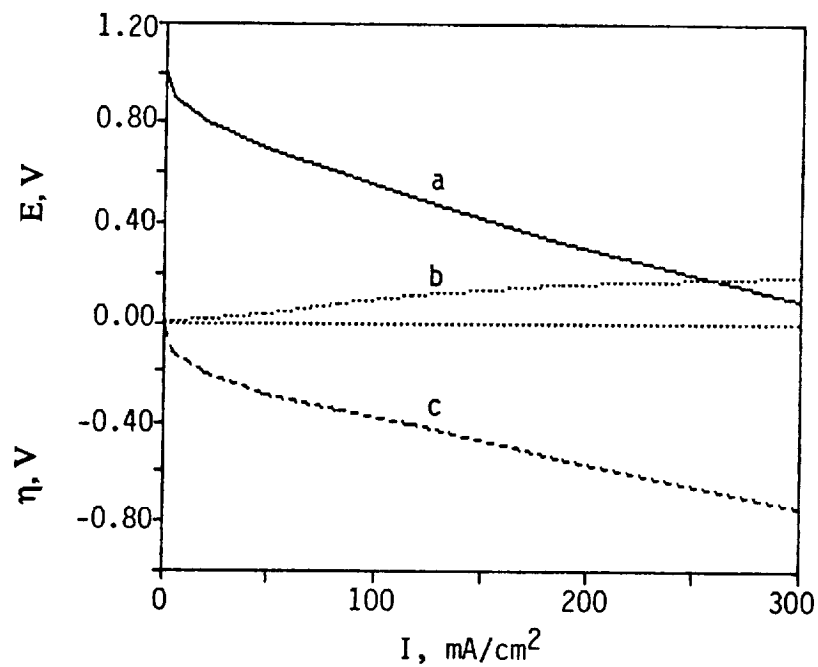


Figure 30. Current voltage behavior of a carbon supported platinum-Nafion structure (Type B). 20°C, 2.0 atm H₂ and O₂. a, cell voltage; b, anode polarization and c, cathode polarization.

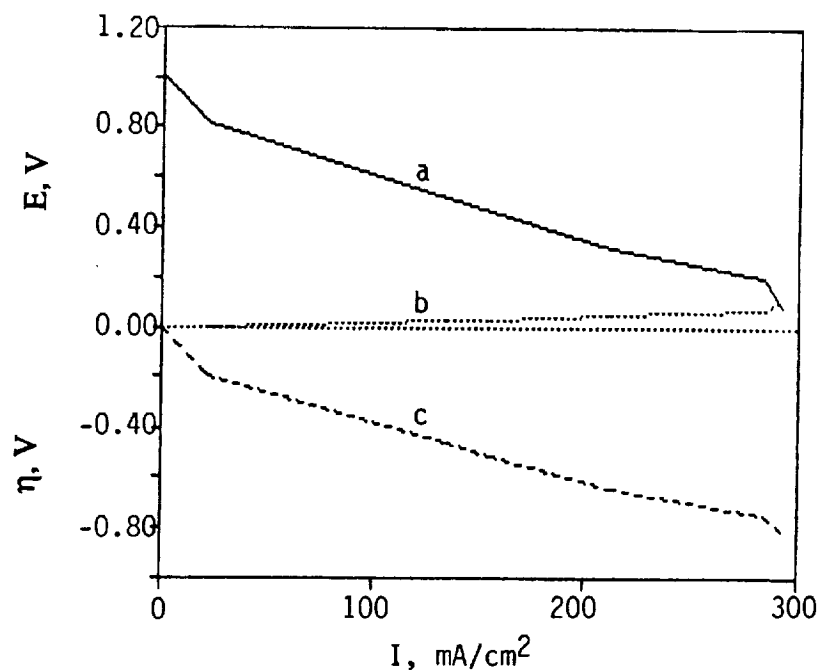


Figure 31. Current voltage behavior of a carbon supported platinum-Nafion structure (Type B). 50°C, 1.3 atm H₂ and O₂. a, cell voltage; b, anode polarization and c, cathode polarization.

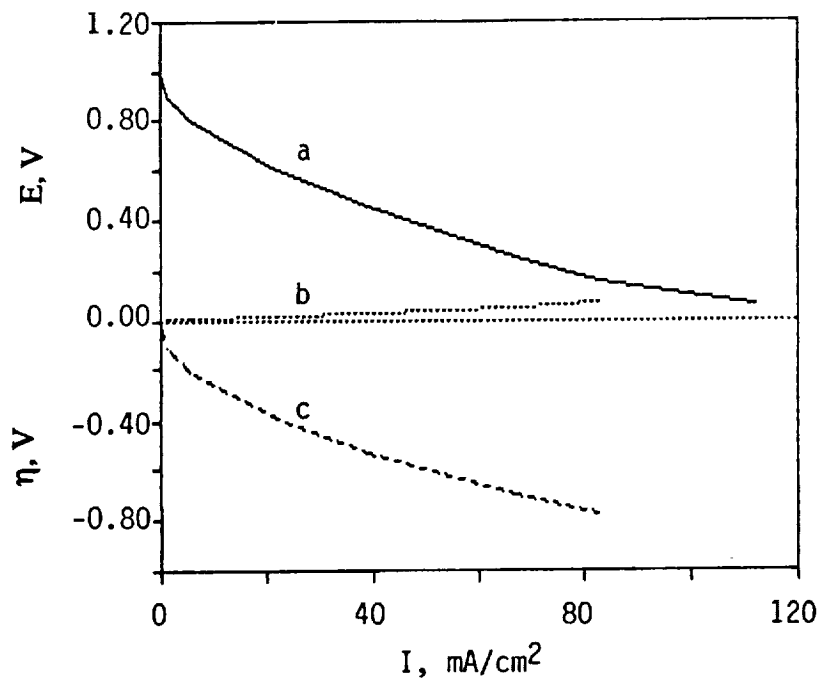


Figure 32. Current voltage behavior of a carbon supported platinum-Nafion structure (Type B). 20°C, 1.3 atm H₂ and O₂. a, cell voltage; b, anode polarization and c, cathode polarization.

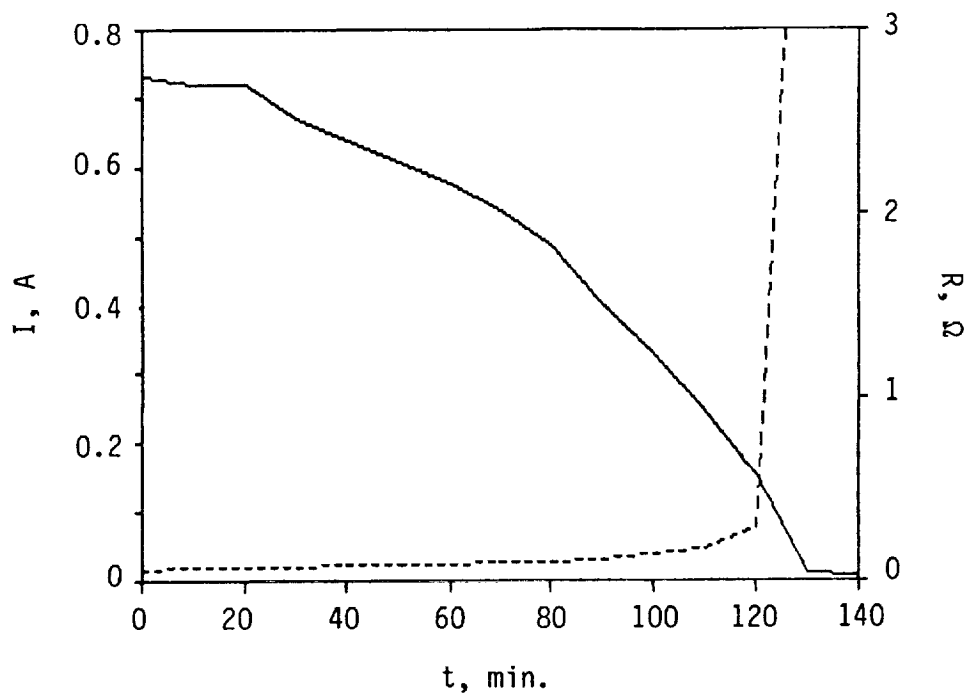


Figure 33. Cell current and resistance at a constant cell voltage of 0.55V during dehydration of a carbon supported platinum-Nafion structure (Type B). 50°C, 1.3 atm H₂ and O₂. O₂ flow rate = 160 cm³/min.

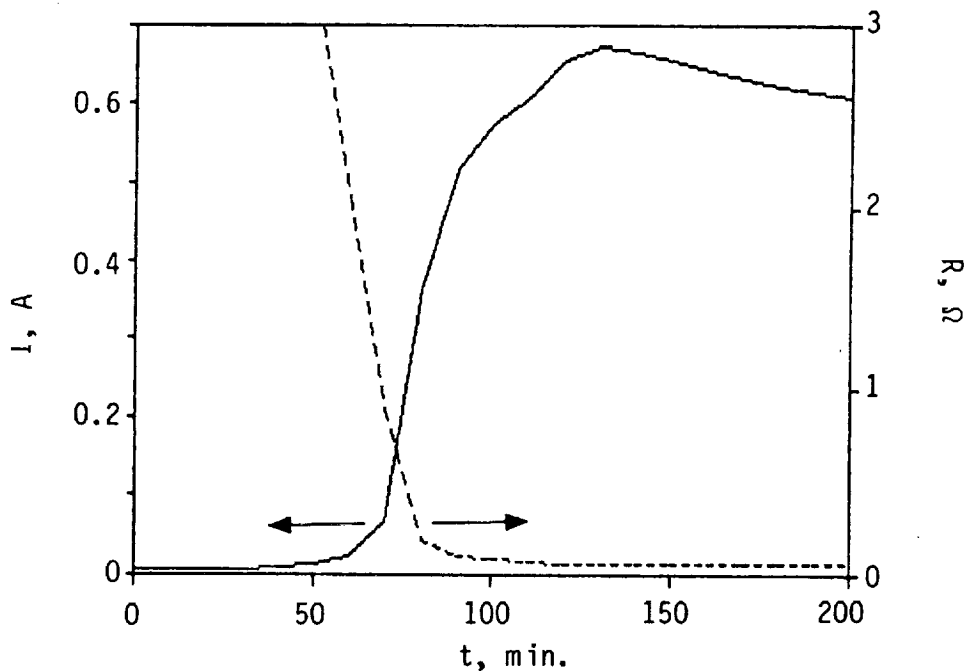


Figure 34. Cell current and resistance at a constant cell voltage of 0.55V during self rehydration of a carbon supported platinum-Nafion structure (Type B). 20°C, 1.3 atm H₂ and O₂. O₂ bleed rate = 10 cm³/min after 75 min.

3.3 Discussion and Conclusions

Stable fuel cell operation without gas humidification means that there can be no net transfer of water across the cell. This requires a gradient in water activity and by necessity less than full hydration at the anode. To achieve the maximum possible hydration at the cathode we must maintain a thin film of liquid water to fill the micropores of the semi-hydrophobic membrane. This water film needs to remain extremely thin to avoid oxygen transport limitations, a common phenomenon of "electrode flooding". Our investigation showed that such conditions can in fact be achieved with well integrated electrode-membrane structures. We have self started cells with completely dry membranes and with dry gases at room temperature. Subsequently, the cells were operated on dry gases for extended time with stable performance. Typical room temperature low pressure operation yielded 100 mA/cm^2 at 0.5V and maximum currents over 300 mA/cm^2 . This is a remarkable performance considering the relatively poor electrode structures fabricated during this initial feasibility investigation. Electrode thickness, catalyst loading and catalyst distribution were far from what we expect from an optimum structure. Electrode polarization and in particular polarization at the cathode was limiting in most cases. Additional studies are necessary to identify the detailed nature of the limiting process or combination of processes. Only then can we make meaningful projections of the ultimate fuel cell performance which might be achieved at ambient or near ambient conditions without gas conditioning.

In summary we can draw the following conclusions:

- PEM fuel cells can operate at ambient temperature on unhumidified gases.
- A dry PEM fuel cell can self start improving its performance as reaction water is generated.
- Cell performance is limited by the electrode rather than by membrane resistance.
- Integral membrane-platinum electrode units are feasible and perform attractively. Electrode structure is performance limiting and requires optimization.

4.0 REFERENCES

1. S. Srinivasan, "Fuel Cells for Extraterrestrial and Terrestrial Applications", *J. Electrochem. Soc.*, **136**, (1989) 410.
2. E. A. Ticianelli, C. R. Derouin and S. Srinivasan, "Localization of Platinum in Low Catalyst Loading Electrodes to Attain High Power Densities in SPE Fuel Cells", *J. Electroanal. Chem.*, **251** (1988) 275.
3. S. Srinivasan, E. A. Ticianelli, C. R. Devouin and A. Redondo, "Advances in Solid Polymer Electrolyte Fuel Cell Technology with Low Platinum Loading Electrodes", *J. Power Sources*, **22** (1988) 359.
4. S. Srinivasan, A. Parthasarathy, O. A. Velev, A. C. Ferreira, S. Mukerjee and A. J. Appleby, "Recent Advances in Proton Exchange Membrane Fuel Cell Technology," Proc. "Structural Effects in Electrocatalysis and Oxygen Electrochemistry", **PV92-11**, p. 474, The Electrochem. Soc., Pennington, NJ (1992).
5. T. E. Springer and S. Gottesfeld, "Pseudohomogeneous Catalyst Layer Model for Polymer Electrolyte Fuel Cells", **PV91-10**, p. 197, The Electrochemical Society, Pennington, NJ (1991).
6. T. A. Zawodzinski, Jr., C. Derouin, S. Radzinski, R. J. Sherman, V. T. Smith, T. E. Springer and S. Gottesfeld, "Water Uptake by and Transport Through Nafion® 117 Membranes", *J. Electrochem. Soc.*, **140**, 1041 (1993).
7. S. Srinivasan, A. Parthasarathy, O. A. Velev, A. C. Ferreira, S. Mukerjee and A. J. Appleby, "Recent Advances in Proton Exchange Membrane Fuel Cell Technology," Proc. "Structural Effects in Electrocatalysis and Oxygen Electrochemistry", **PV92-11**, p. 474, The Electrochem. Soc., Pennington, NJ (1992).
8. T. F. Fuller and J. Newman, "Water and Thermal Management in Solid-Polymer Electrolyte Fuel Cells", *J. Electrochem. Soc.*, **140**, 1218 (1993).
9. T. A. Zawodzinski, Jr. M. Newman, L. O. Sillerud and S. Gottesfeld, "Determination of Water Diffusion Coefficients in Perfluorosulfonate Ionomeric Membranes", *J. Phys. Chem.*, **95**, 6040 (1991).
10. T. A. Zawodzinski, Jr., T. E. Springer, J. Davey, J. Valerio and S. Gottesfeld, "Water Transport Properties of Fuel Cell Ionomers", Proc. "Modeling of Batteries and Fuel Cells", **PV91-90**, p. 187, Electrochem. Soc., Pennington, NJ 1991.
11. F. A. Uribe, M. S. Wilson, T. E. Springer and S. Gottesfeld, "Oxygen Reduction (ORR) at the Pt/Recast Ionomer Interface and Some General Comments on ORR at PT/Aqueous Electrolyte Interfaces", Proc. Structural Effects in Electrocatalysis and Oxygen Electrochemistry", **PV92-11**, p. 494, The Electrochemical Society, Pennington, NJ (1992).
12. T. E. Springer, T. A. Zawodzinski and S. Gottesfeld, "Modeling Water Content Effects in Polymer Electrolyte Fuel Cells, **PV91-90**, p. 209, Electrochem. Soc., Pennington, NJ 1991.
13. H. Koch, A. Nandi, N. K. Anand, O. Velev, D. H. Swan, S. Srinivasan and A. J. Appleby, "Water Transport Across the Membrane in Solid Polymer Electrolyte Fuel Cell", Ext. Abstract No. 115, Electrochemical Society, Seattle (1990).

14. P. Staiti, Z. Poltavzewski, V. Alderucci, G. Maggio, N. Giordano and A. Fasulo, "Influence of Electrode Properties on Water Management in a Solid Polymer Electrolyte Fuel Cell", *J. Appl. Electrochem.*, 22 (1992) 633.
15. F. A. Uribe, T. E. Springer and S. Gottesfeld, "A Microelectrode Study of Oxygen Reduction at the Platinum Recast Nafion Film Interface", *J. Electrochem. Soc.*, 139 (1992) 765.
16. E. A. Ticianelli, C. R. Derouin, A. Redondo and S. Srinivasan, "Methods to Advance Technology of Proton Exchange Membrane Fuel Cells", *J. Electrochem. Soc.*, 135 (1988) 2209.
17. P. Millet, M. Pineri and R. Durand, "New Solid Polymer Electrolyte Composites for Water Electrolysis", *J. Appl. Electrochem.*, 19, (1989) 162.
18. P. Millet, T. Alleau, R. Durand, "Characterization of Membrane-Electrode Assemblies for Solid Polymer Electrolyte Water Electrolyzers", *J. Appl. Electrochem.*, 23, 322 (1993).